

Exploration of immunoglobulin transcriptomes from mice immunized with three-finger toxins and phospholipases A₂ from the Central American coral snake, *Micrurus nigrocinctus*

Andreas H Laustsen ^{Corresp., 1,2}, Mikael Engmark ^{1,3}, Christopher Clouser ⁴, Sonia Timberlake ⁵, Francois Vigneault ^{4,6}, José María Gutiérrez ⁷, Bruno Lomonte ⁷

¹ Department of Biotechnology and Biomedicine, Technical University of Denmark, Kgs. Lyngby, Denmark

² Department of Drug Design and Pharmacology, University of Copenhagen, Copenhagen, Denmark

³ Department of Bio and Health Informatics, Technical University of Denmark, Kgs. Lyngby, Denmark

⁴ Juno Therapeutics, Seattle, Washington, United States of America

⁵ Finch Therapeutics, Somerville, Massachusetts, United States of America

⁶ AbVitro, Boston, MA, United States of America

⁷ Instituto Clodomiro Picado, Universidad de Costa Rica, San José, Costa Rica

Corresponding Author: Andreas H Laustsen

Email address: ahola@bio.dtu.dk

Snakebite envenomings represent a neglected public health issue in many parts of the rural tropical world. Animal-derived antivenoms have existed for more than a hundred years and are effective in neutralizing snake venom toxins when timely administered. However, the low immunogenicity of many small but potent snake venom toxins represents a challenge for obtaining a balanced immune response against the medically relevant components of the venom. Here, we employ next generation sequencing of the immunoglobulin (Ig) transcriptome of mice immunized with a three-finger toxin and a phospholipase A₂ from the venom of the Central American coral snake, *Micrurus nigrocinctus*. Results showed that only low frequencies of mRNA encoding IgG isotypes, the most relevant isotype for therapeutic purposes, were present in splenocytes of mice immunized with 6 doses of the toxins over 90 days. Furthermore, analysis of Ig heavy chain transcripts showed that no particular combination of variable (V) and joining (J) gene segments had been selected in the immunization process, as would be expected after a strong humoral immune response to a single antigen. Combined with the titration of toxin-specific antibodies in the sera of immunized mice, these data support the low immunogenicity of three-finger toxins and phospholipases A₂ found in elapid snake venoms, and highlight the need for future studies analyzing the complexity of antibody responses to toxins at the molecular level.

1

2 Exploration of immunoglobulin transcriptomes from mice immunized with three-

3 finger toxins and phospholipases A₂ from the Central American coral snake,4 *Micrurus nigrocinctus*

5

6 Andreas H. Laustsen^{1,2*}, Mikael Engmark^{1,3}, Christopher Clouser⁴, Sonia Timberlake⁴, Francois7 Vigneault⁴, José María Gutiérrez⁵, Bruno Lomonte⁵

8

9 ¹ Department of Biotechnology and Biomedicine, Technical University of Denmark, Denmark10 ² Department of Drug Design and Pharmacology, Faculty of Health and Medical Sciences,
11 University of Copenhagen, Denmark12 ³ Department of Bio and Health Informatics, Technical University of Denmark, Denmark13 ⁴ Juno Therapeutics, Seattle (WA), USA14 ⁵ Instituto Clodomiro Picado, Facultad de Microbiología, Universidad de Costa Rica,
15 San José, Costa Rica

16

17 **Running title:** Antibody isotyping of immune response against coral snake toxins

18

19 **Keywords:** *Micrurus nigrocinctus*; coral snake; venom; toxins; murine immune response;
20 antibodies; antibody isotyping; next generation sequencing; antivenom

21

22 *** Address correspondence to:**

23

24 Dr. Andreas H. Laustsen (ahola@bio.dtu.dk), Department of Biotechnology and Biomedicine,
25 Technical University of Denmark, Denmark

26

28 **Abstract**

29 Snakebite envenomings represent a neglected public health issue in many parts of the rural
30 tropical world. Animal-derived antivenoms have existed for more than a hundred years and are
31 effective in neutralizing snake venom toxins when timely administered. However, the low
32 immunogenicity of many small but potent snake venom toxins represents a challenge for
33 obtaining a balanced immune response against the medically relevant components of the venom.
34 Here, we employ next generation sequencing of the immunoglobulin (Ig) transcriptome of mice
35 immunized with a three-finger toxin and a phospholipase A₂ from the venom of the Central
36 American coral snake, *Micrurus nigrocinctus*. Results showed that only low frequencies of
37 mRNA encoding IgG isotypes, the most relevant isotype for therapeutic purposes, were present
38 in splenocytes of mice immunized with 6 doses of the toxins over 90 days. Furthermore, analysis
39 of Ig heavy chain transcripts showed that no particular combination of variable (V) and joining
40 (J) gene segments had been selected in the immunization process, as would be expected after a
41 strong humoral immune response to a single antigen. Combined with the titration of toxin-
42 specific antibodies in the sera of immunized mice, these data support the low immunogenicity of
43 three-finger toxins and phospholipases A₂ found in elapid snake venoms, and highlight the need
44 for future studies analyzing the complexity of antibody responses to toxins at the molecular
45 level.

46 (232 words)

48 1. Introduction

49 Snakebite envenomings represent a major public health concern in tropical regions of the world
50 (*Williams et al., 2011*). Despite emerging discoveries that may one day pave the way for novel
51 biotechnology-based antivenoms (reviewed by *Laustsen et al., 2016a; 2016b*), animal serum-
52 derived antivenoms remain the cornerstone of snakebite envenoming treatment (*Gutiérrez et al.,*
53 *2011*). Production of antivenom is challenged by a large variation in immunogenicity of many
54 key snake venom toxins resulting in unpredictable immune responses in production animals
55 (*Cook et al., 2010; Guidolin et al., 2010*). It has been shown that many of the immunogenic
56 venom components are in fact not important for toxicity (*Antúnez et al., 2010; Gutiérrez et al.,*
57 *2009; Laustsen et al., 2015*), and conversely, that some highly toxic venom components, such as
58 α -neurotoxins, phospholipases A₂, and P-I snake venom metalloproteinases may be poorly
59 immunogenic (*Schottler, 1951; Gutiérrez et al., 2009; Chotwiwatthanakun et al., 2001; Ownby*
60 *& Colberg, 1990; Judge et al., 2006*). Combined, this creates a challenge for antivenom
61 production, since the goal of obtaining an antivenom with a strong, yet balanced response against
62 all the medically relevant toxins becomes a complex endeavor.

63 Coral snakes (genera *Micrurus*, *Leptomicrurus*, and *Micruroides*) are, together with the sea
64 snake *Hydrophis (Pelamis) platura*, the representatives of the snake family Elapidae in the
65 Americas, comprising approximately 85 species (*Campbell & Lamar, 2004; the Reptile Database*
66 *- www.reptile-database.org*). Although *Micrurus* species are only responsible for about 1-2% of
67 snakebite cases in this continent, envenomings by these snakes can be fatal if not treated properly
68 and timely (*Warrell, 2004; Gutiérrez, 2014; Bucarechi et al., 2016*). Envenomings resulting
69 from coral snakebites are predominantly associated with descending neuromuscular paralysis,
70 which may end in respiratory arrest (*Warrell, 2004; Bucarechi et al., 2016*).

71 Production of antivenoms against *Micrurus* snakes is particularly challenging, as (a) it is
72 very difficult to maintain coral snakes in captivity; (b) the majority of *Micrurus* species provide a
73 very low yield of venom, implying that the collection of the quantities of venom required for
74 horse immunization and quality control testing demands the ‘milking’ of many specimens; and
75 (c) there is a variable extent of immunological cross-recognition between venoms from coral
76 snakes of different species; hence, antivenoms raised against some species are not always
77 effective in the neutralization of venoms of other species (*Bolaños, Cerdas & Abalos, 1978*;
78 *Tanaka et al., 2016*). As a result, only a few laboratories manufacture *Micrurus* antivenoms, and
79 several countries where these snake inhabit completely lack this therapeutic resource, which
80 severely limits the clinical management of these accidents.

81 Knowledge on the composition of the venoms of *Micrurus* species has increased steadily
82 over the last years, as a consequence of proteomic characterizations (reviewed by *Lomonte et al.,*
83 *2016b*). Two main venom phenotype patterns have been identified, i.e. venoms rich in
84 neurotoxins of the three-finger toxin (3FTx) family, and venoms rich in phospholipases A₂
85 (PLA₂s) (*Fernández et al., 2015*). In addition to these two main protein families, other minor
86 components of these venoms include L-amino acid oxidases, serine proteinases,
87 metalloproteinases, nerve growth factor, C-type lectin-like proteins, Kunitz-type inhibitors,
88 among others (*Fernández et al., 2011, 2015; Corrêa-Netto et al., 2011; Lomonte et al., 2016a;*
89 *Sanz et al., 2016; Rey-Suárez et al., 2011, 2016*). In some cases, the toxins playing the main role
90 in overall toxicity have been identified (*Rey-Suárez et al., 2012; Vergara et al., 2014; Fernández*
91 *et al., 2015; Castro et al., 2015; Ramos et al., 2016*).

92 The limited immunogenicity of the highly toxic PLA₂s and 3FTxs (*Fernández et al.,*
93 *2011, Rosso et al., 1996; Alape-Girón et al., 1996*) represents another difficulty in production of

94 *Micrurus* antivenom, since it thwarts the goal of raising a balanced immune response against
95 these medically relevant toxins. In order to further explore how these toxins interact with the
96 mammalian immune system, we chose a mouse model and employed an NGS approach using the
97 AbSeq™ technology developed by AbVitro (now Juno Therapeutics,
98 <https://www.junotherapeutics.com>), based on Illumina sequencing. The methodology was
99 utilized to sequence immunoglobulin (Ig) encoding mRNA transcripts from splenic B-
100 lymphocytes in mice subjected to immunization with either a 3FTx or a PLA₂ toxin from the
101 venom of *M. nigrocinctus* (Central American coral snake). By this approach, the transcription
102 levels of different immunoglobulin isotypes and dominant clones of B-lymphocytes with a
103 particular usage of V (variable) and J (joining) gene segments can be determined for Ig heavy
104 chain transcripts. This methodology has previously been employed for investigating B-cell
105 populations in autoimmune (*Stern et al., 2014*) or infectious diseases (*Tsioris et al., 2015; Di*
106 *Niro et al., 2015*), for example. By employing the AbSeq™ high-throughput approach, we
107 explore, for the first time, the Ig transcriptome including VJ usage patterns in individual animals
108 subjected to immunization with two relevant toxin classes of elapid snakes. This study thus
109 provides novel insight into the humoral response of mice immunized with 3FTx or PLA₂ toxins
110 and highlights important challenges of raising antibodies against poorly immunogenic toxins.

111

112 **2. Materials and Methods**

113 *2.1 Snake venom and toxins*

114 Venom from *M. nigrocinctus* was obtained from a pool of more than 50 specimens collected in
115 the Central Pacific region of Costa Rica, kept at the serpentarium of Instituto Clodomiro Picado,
116 Universidad de Costa Rica. The venom was lyophilized and stored at -20°C.

117 Fractionation of the venom was performed by RP-HPLC on a C₁₈ column (4.6 x 250 mm, 5
118 µm particle diameter; Supelco) as previously described (*Fernández et al., 2011*). In brief, 2 mg
119 of venom dissolved in 200 µL of water containing 0.1% trifluoroacetic acid (TFA; solution A)
120 were separated at 1 mL/min in an Agilent 1200 chromatograph monitored at 215 nm, applying a
121 gradient towards solution B (acetonitrile, containing 0.1% TFA): 0% B for 5 min, 0–15% B over
122 10 min, 15–45% B over 60 min, 45–70% B over 10 min, and 70% B over 9 min. Fractions of
123 interest were collected manually, dried in a vacuum centrifuge, and identified by trypsin
124 digestion followed by MALDI-TOF/TOF mass spectrometry (*Fernández et al., 2011*). Proteins
125 were redissolved in water and their concentrations were estimated on the basis of their
126 absorbance at 280 nm, using a NanoDrop (Thermo) instrument.

127

128 *2.2 Immunization of mice*

129 Three CD-1 mice were immunized with a three-finger toxin (3FTx), and two with a
130 phospholipase A₂ (PLA₂), respectively. These correspond to fractions #3 (~P80548) and #30
131 (~P81166/P81167) described in the previous proteomic characterization of this venom
132 (*Fernández et al., 2011*). All toxin doses were injected by the intraperitoneal route. The priming
133 dose was 1 µg emulsified in Freund's complete adjuvant, followed by five booster doses injected
134 in physiological saline without adjuvant, at days 15 (1 µg), 43 (2 µg) 63 (4 µg), and 83 (6 µg for
135 the 3FTx and 8 µg for the PLA₂). At day 90, after obtaining a blood sample for monitoring of the
136 antibody response by enzyme-immunoassay, mice were euthanized by CO₂ inhalation. Their
137 spleens were immediately removed, cut in small pieces, and disaggregated over a stainless steel
138 mesh to obtain splenocytes. These cell suspensions were aliquoted in RNeasy[®] solution
139 (Thermo) and shipped within 24 h to AbVITro, at room temperature, for subsequent molecular

140 studies. The use of animals for these experiments followed the ethical guidelines of the *Comité*
141 *Institucional para el Uso y Cuido de Animales* (CICUA), Universidad de Costa Rica, with the
142 approval number 82-08.

143

144 *2.3 Enzyme-immunoassay (ELISA)*

145 In order to evaluate the individual antibody responses of the mice, wells in MaxiSorp 96-well
146 plates (NUNC, Roskilde, Denmark) were coated overnight with 1 μg of either 3FTx or PLA₂,
147 dissolved in 100 μL PBS (0.12 M NaCl, 0.04 M sodium phosphate, pH 7.2). Wells were washed
148 five times with PBS and blocked by adding 100 μL PBS containing 2% (w:v) bovine serum
149 albumin (BSA, Sigma), and incubated at room temperature for 1 h. Plates were then washed five
150 times with PBS. Serial dilutions of serum from each mouse were prepared in PBS + 2% BSA
151 and 100 μL was added to each well, in triplicates, and incubated overnight at 4°C. Normal mouse
152 serum, run simultaneously under identical conditions was used as a control for background.
153 Plates were then washed five times with PBS, followed by the addition of 100 μL of a 1:3000
154 dilution of anti-mouse IgG (whole molecule) antibodies conjugated to alkaline phosphatase, in
155 PBS + 1% BSA. The plates were incubated for 2 h, and then washed five times with FALC
156 buffer (0.05 M Tris, 0.15 M NaCl, 20 μM ZnCl₂, 1 mM MgCl₂, pH 7.4). Development of color
157 was attained by addition of 100 μL *p*-nitrophenyl phosphate (1 mg/mL in 9.7% v/v
158 diethanolamine buffer, pH 9.8) and absorbances at 405 nm were recorded (Multiskan FC,
159 Thermo Scientific).

160 *2.4 Assessment of mRNA quality*

161 Assessment of RNA quality was performed using Agilent's TapeStation according to the
162 manufacturers protocol and algorithm to calculate RIN^e scores

163 (<http://www.agilent.com/cs/library/technicaloverviews/public/5990-9613EN.pdf>).

164

165 *2.5 Library preparation and high-throughput sequencing of B-cell receptors*

166 The method for high-throughput sequencing of the B-cell repertoire was performed as described
167 elsewhere (*Di Niro et al., 2015; Tsioris et al., 2015*). Briefly, RNA was reverse-transcribed into
168 cDNA using a biotinylated oligo dT primer. An adaptor sequence was added to the 3' end of all
169 cDNA, which contains the Illumina P7 universal priming site and a 17-nucleotide unique
170 molecular identifier (UMI). Products were purified using streptavidin-coated magnetic beads
171 followed by a primary PCR reaction using a pool of primers targeting the IGHA, IGHD, IGHE,
172 IGHG, IGHM, IGKC and IGLC regions, as well as a sample-indexed Illumina P7C7 primer. The
173 immunoglobulin-specific primers contained tails corresponding to the Illumina P5 sequence.
174 PCR products were then purified using AMPure XP beads. A secondary PCR was then
175 performed to add the Illumina C5 clustering sequence to the end of the molecule containing the
176 constant region. The number of secondary PCR cycles was tailored to each sample to avoid
177 entering plateau phase, as judged by a prior quantitative PCR analysis. Final products were
178 purified, quantified with Agilent TapeStation and pooled in equimolar proportions, followed by
179 high-throughput paired-end sequencing on the Illumina MiSeq platform. For sequencing, the
180 Illumina 600 cycle kit was used with the modifications that 325 cycles was used for read 1, 6
181 cycles for the index reads, 300 cycles for read 2 and a 10% PhiX spike-in to increase sequence
182 diversity.

183

184 *2.6 VJ repertoire sequencing data analysis*

185 MiSeq reads were demultiplexed using Illumina software, and processed with the pRESTO

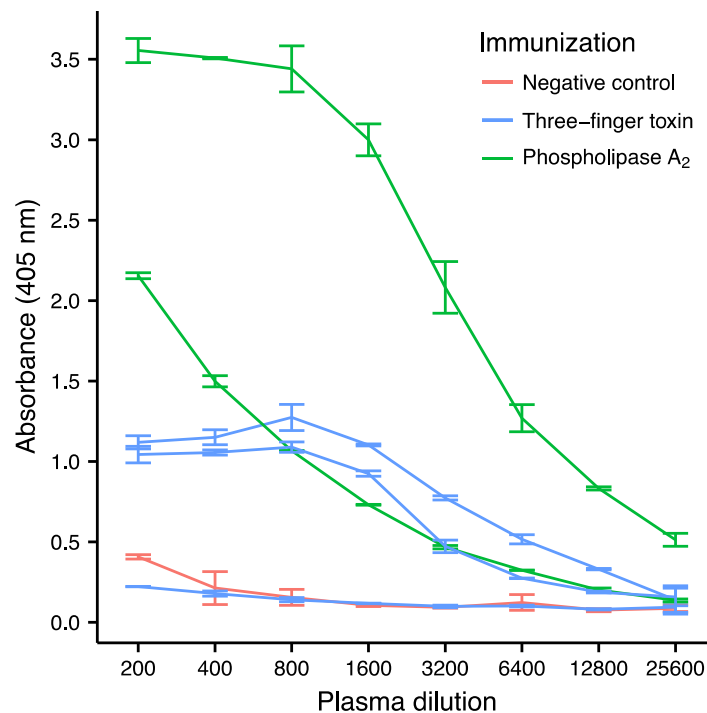
186 toolsuite (*Vander Heiden et al., 2014*) as following: Positions with less than Phred quality 5 were
187 masked with Ns. Isotype-specific primers and molecular barcodes (UIDs or UMIs) were
188 identified in the amplicon and trimmed, using pRESTO MaskPrimers-cut. A read 1 and read 2
189 consensus sequence was generated separately for each mRNA from reads grouped by unique
190 molecular identifier, which are PCR replicates arising from the same original mRNA molecule of
191 origin. UMI read groups were aligned with MUSCLE (*Edgar, 2004*), and pRESTO was used to
192 BuildConsensus, requiring $\geq 60\%$ of called PCR primer sequences agree for the read group,
193 maximum nucleotide diversity of 0.1, using majority rule on indel positions, and masking
194 alignment columns with low posterior (consensus) quality. Paired end consensus sequences were
195 then stitched in two rounds. First, ungapped alignment of each read pair's consensus sequence
196 termini was optimized using a Z-score approximation and scored with a binomial p -value as
197 implemented in pRESTO AssemblePairs-align. For read pairs failing to stitch this way, stitching
198 was attempted using the human BCR germline V exons to scaffold each read prior to stitching or
199 gapped read-joining, using pRESTO's AssemblePairs-reference. Positions with posterior
200 consensus quality less than Phred 5 were masked again with Ns. Each mRNA was annotated for
201 V, D, J germline gene of origin, productivity, and CDR3 region using igblastn (*Ye et al., 2013*).
202 Annotated data were analyzed with custom scripts and visualized with R (*R Core Team, 2014*).
203 Clones were defined using a conservative approach, grouping mRNAs from the same V and J
204 germline gene of origin and having the same isotype and CDR3 sequence.

205

206 **3. Results and Discussion**

207 Three-finger toxins (3FTx) and phospholipase A₂s (PLA₂) are the two most abundant toxin
208 families in the venom of *M. nigrocinctus* (*Fernández et al., 2011*), and generally they are the two

209 snake toxin families which have been most investigated (*Laustsen et al., 2016a*). In the venom of
210 *M. nigrocinctus* these toxins cause neuromuscular paralysis, owing to a combination of pre- and
211 post-synaptic actions, and myotoxicity, providing the venom with its high toxicity (*Rosso et al.,*
212 *1996; Alape-Girón et al., 1996*). In previous studies it was observed that 3FTxs and PLA₂s were
213 recognized more weakly than larger proteins from this venom, by a therapeutic equine antivenom
214 (*Fernández et al., 2011*). Despite their low immunogenicity, it was possible to raise an antibody
215 response against both toxins in four out of five mice, although high variation in the antibody titer
216 was observed (*Fig. 1*). Mice immunized with PLA₂ had a higher antibody titer than mice
217 immunized with the 3FTx, in agreement with the higher molecular mass of the former.
218



219

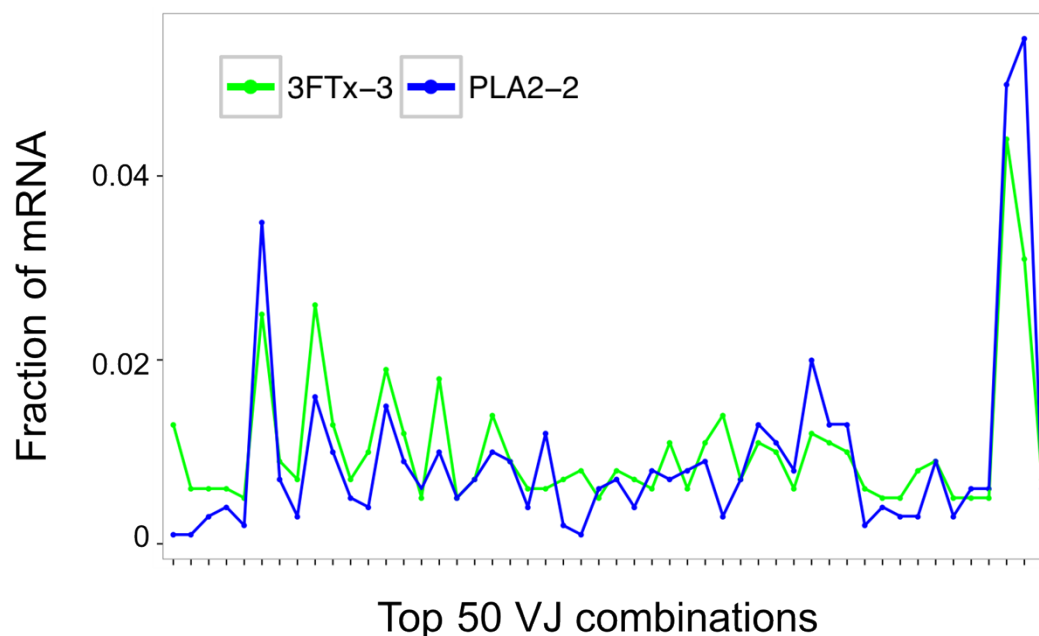
220 **Figure 1:** ELISA titrations of serum antibodies against *M. nigrocinctus* PLA₂ or 3FTx in mice.

221 Two mice were immunized with PLA₂, and three were immunized with 3FTx. Plates were coated

222 with either PLA₂ or 3FTx, and antibodies were detected as described in Materials and Methods.

223

224 Assessment of the mRNA from harvested mouse splenocytes indicated that it was of sufficient
225 quality to proceed to sequencing (RIN^e scores between 5.2 and 6.4). A next generation
226 sequencing approach (AbSeq™) was employed to investigate transcription levels of Ig isotypes
227 and the usage of V and J gene segments for heavy chain assembly in mice that were immunized
228 with a 3FTx or a PLA₂. Investigation of the 50 most frequent VJ combinations for the
229 immunized mice did not, however, result in identification of a dominant combination, as the VJ
230 usage was found to be similar across all samples (Fig. 2). This finding suggests that the
231 generated antibody responses might be diverse and that multiple specific antibodies with low
232 abundance are generated in each mouse.



233

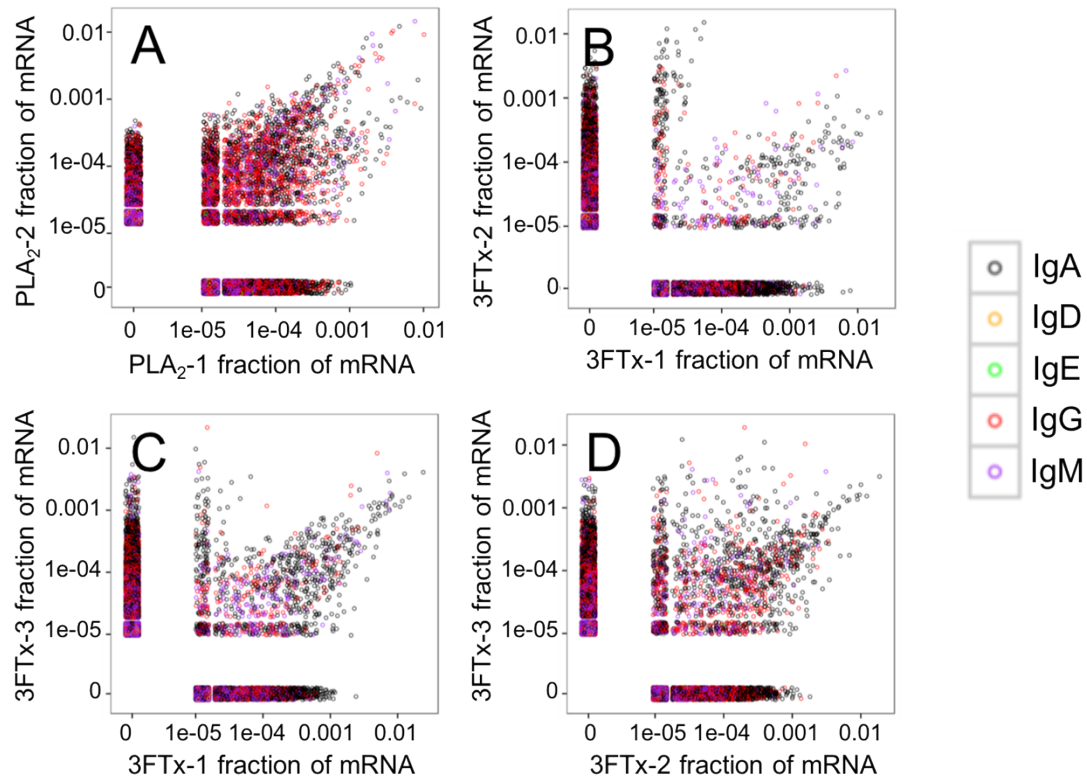
234

235 **Figure 2.** Comparison of the relative abundance of mRNA for the 50 most abundant VJ
236 combinations for the mouse 3FTx-3 and mouse PLA₂-2 showing VJ usage to be similar across
237 samples. Similar VJ usage patterns were observed for other pairs of immunized mice (data not
238 shown).

239

240 Looking at the sequences of all mRNA transcripts encoding heavy chain variable domain (V_H)
241 clones across each sample, we were able to find shared V_H clones with similar relative
242 abundances in either the PLA₂-immunized or the 3FTx-immunized mice (Fig. 3). In comparison,
243 almost no V_H clones were shared between mice immunized with different toxins (Fig. 4). This
244 implies that the immunization procedure did indeed elicit specific, but different responses
245 dependent on whether PLA₂s or 3FTxs were employed for immunization. The relatively high
246 number of V_H clones found in both of the PLA₂-immunized mice (Fig. 3A) compared to lower
247 number of V_H clones found across the three 3FTx-immunized mice (Fig. 3B-D) further indicate
248 that immunization with PLA₂s is more prone to give rise to antibodies transcribed in similar
249 quantities. Also, an intermediate number of similar V_H clones was found in both the PLA₂-1 and
250 3FTx-3 samples (Fig. 4E), even though the correlation in relative abundance was not equally
251 pronounced. This is likely explained by the fact that the majority of V_H clones found in both
252 PLA₂-immunized mice are not expected to be specific towards the toxins, but instead are likely to
253 be directed against other antigens.

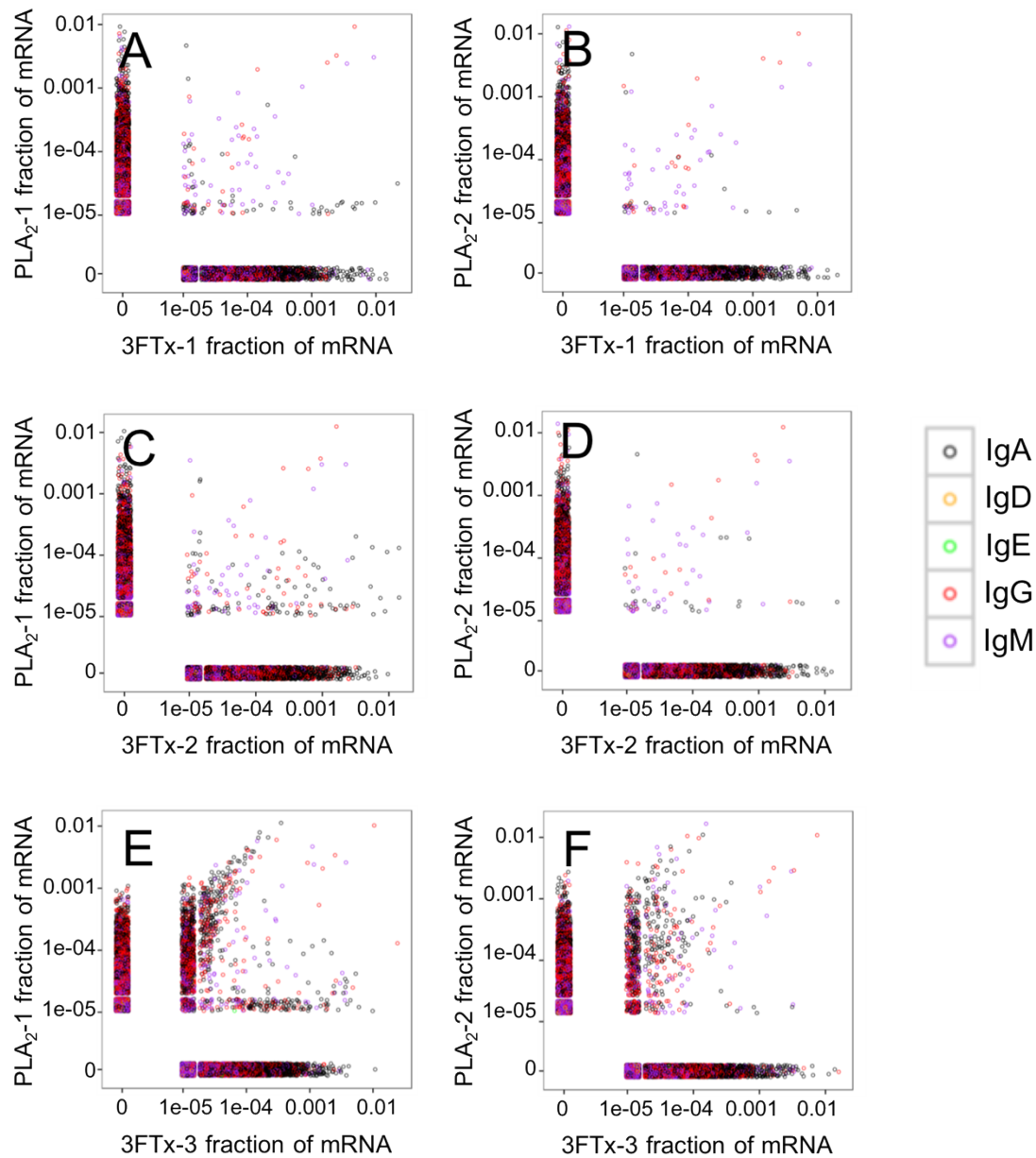
254



255

256 **Figure 3:** Relative abundance of unique V_H clone transcripts compared between samples. A
 257 large group of V_H transcripts are found in similar abundance in different mice immunized with
 258 the same toxin. **A)** Comparison between mouse PLA_2-1 and PLA_2-2 , **B)** Comparison between
 259 mouse $3FTx-1$ and $3FTx-2$, **C)** Comparison between mouse $3FTx-1$ and $3FTx-3$, **D)** Comparison
 260 between mouse $3FTx-2$ and $3FTx-3$.

261



262

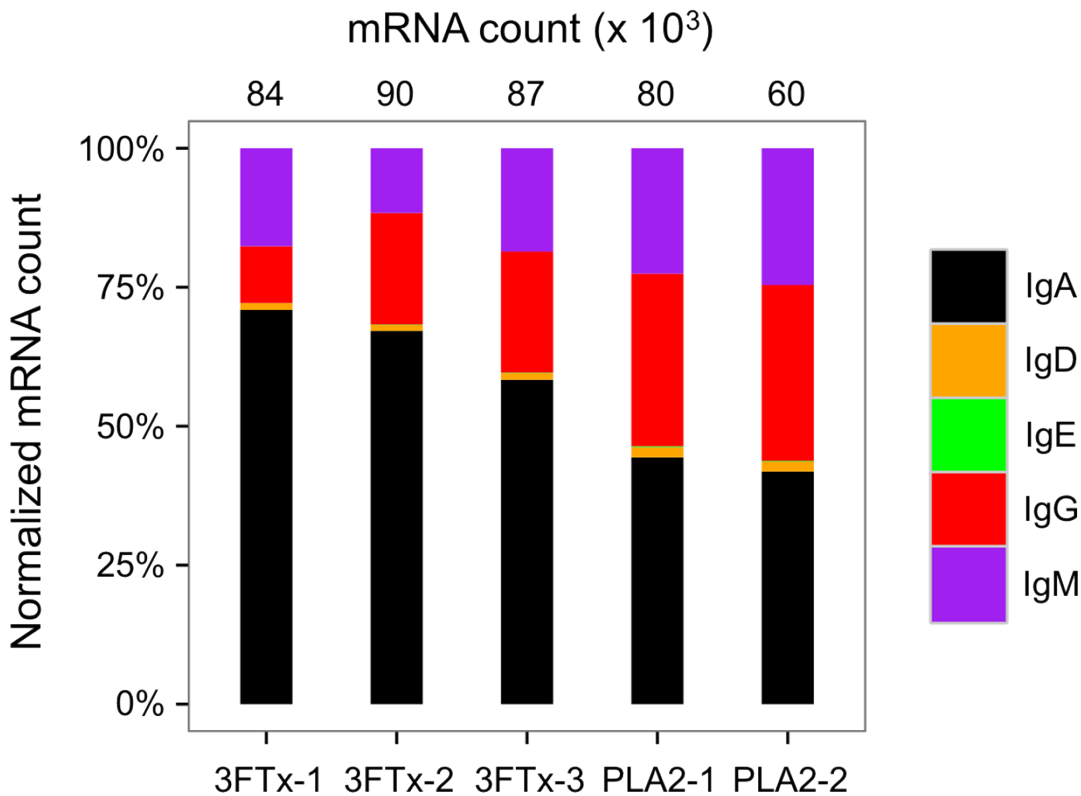
263 **Figure 4:** Relative abundance of unique V_H clone transcripts compared between samples. Only
 264 few V_H transcripts are found in similar abundance in more than one mouse, when mice
 265 immunized with different toxins are compared. **A)** Comparison between mouse PLA₂-1 and
 266 3FTx-1, **B)** Comparison between mouse PLA₂-2 and 3FTx-1, **C)** Comparison between mouse
 267 PLA₂-1 and 3FTx-2, **D)** Comparison between mouse PLA₂-2 and 3FTx-2, **E)** Comparison
 268 between mouse PLA₂-1 and 3FTx-3, **F)** Comparison between mouse PLA₂-2 and 3FTx-3.

269

270 The AbSeq™ antibody sequencing methodology is capable of determining the Ig isotype of the
271 identified V_H clones. The coloring of the V_H clones in [Fig. 3](#) and [Fig. 4](#) reveals that a large
272 number of the most abundant V_H clones present in the mice are of the IgA isotype, which was
273 confirmed by further investigation of all mRNA transcripts from the splenocytes ([Fig. 5](#)). This is
274 surprising, as IgG is known to be the dominant immunoglobulin class in mouse blood after the
275 response to T-dependent protein antigens. The observation could, however, be explained by
276 differences in expression levels due to different translation rates and half-lives of mRNA
277 transcripts encoding different immunoglobulin isotypes. All approved antibody-based therapies
278 on the market are based on IgGs ([Walsh, 2014](#)), which are also the desired isotype for
279 antivenoms. In immunized horses for antivenom production, two isotypes of IgG are largely
280 responsible for the neutralization of toxic effects in the case of viperid snake venoms ([Fernandes
281 et al., 2000](#)). However, analysis of the transcripts obtained from the immunized mice revealed
282 only a low percentage of IgG transcripts, as compared to the transcripts for other Igs ([Figs. 3-5](#)).
283 This finding may indicate a difficulty in raising potent IgG antibodies against both 3FTxs and
284 PLA₂s. Our results may further suggest that the immune response is slightly lower against 3FTxs
285 than for PLA₂s based on the lower abundance of IgG transcripts in mice immunized with 3FTx
286 ([Fig. 5](#)). Taken together with the results from the ELISA assay ([Fig. 1](#)) and the observation that
287 immunization with PLA₂s is more prone to give rise to similar Ig transcripts ([Fig. 3A](#) vs. [Fig.
288 3B-D](#)), we suggest that the PLA₂ toxins are slightly more immunogenic than the 3FTx, although
289 neither toxin seems to have high immunogenicity. The underlying reason for this could possibly
290 be due to the smaller molecular size of 3FTx compared to PLA₂s, or that PLA₂s may contain
291 distinct epitopes better capable of eliciting an adaptive immune response than 3FTxs. This is

292 further supported by the fact that only two IgG-encoding mRNA transcripts are found in the top
293 20 most abundant Ig-encoding mRNA transcripts for only one out of three of the 3FTx-
294 immunized mice. In comparison, six and nine of the top 20 mRNA transcripts for mice
295 immunized with PLA₂s encode the IgG isotype (Fig. 6). It would be interesting to assess whether
296 the immune response of horses against these elapid venom toxins is also characterized by a low
297 proportion of IgG – a finding that would have evident implications for antivenom manufacture.
298 However, this is beyond the scope of this exploratory study.

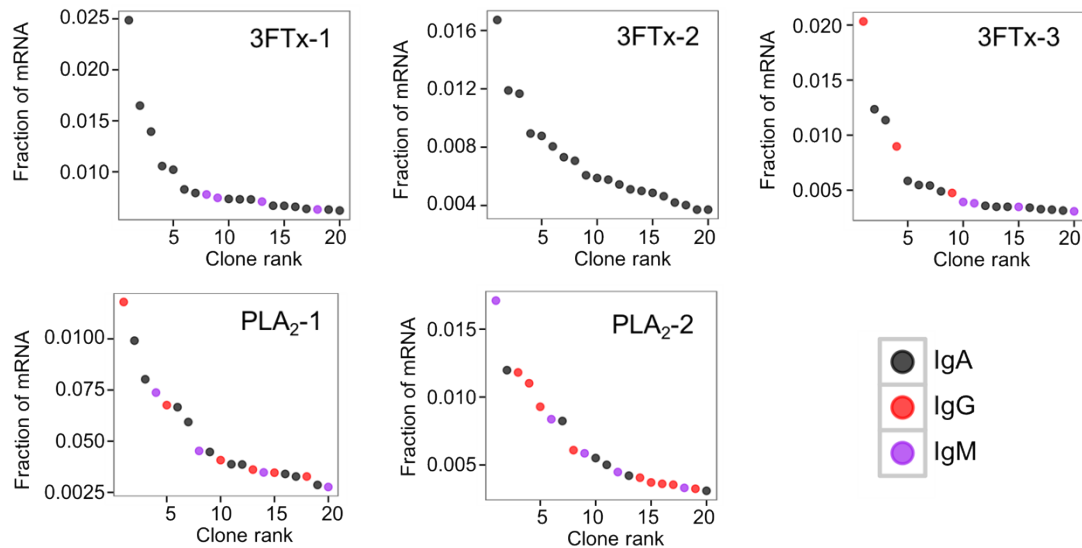
299



300

301 **Figure 5:** Overview of total mRNA transcripts encoding different immunoglobulin isotypes from
302 the immunized mice (normalized). Numbers above each bar represents the mRNA count in each
303 sample.

304



305

306 **Figure 6:** The 20 most abundant V_H clone transcripts and their corresponding isotypes in each
 307 immunized mouse based on their fraction of total immunoglobulin mRNA.

308

309 4. Concluding remarks and outlook

310 In addition to demonstrating the power of the next generation sequencing technology,
 311 AbSeq™, for investigation of immune responses in animals immunized with snake venom
 312 toxins, the findings presented here highlight difficulties in obtaining an IgG response against the
 313 medically important toxins of the 3FTx and PLA₂ families. Given that these proteins play key
 314 toxic roles in envenomings by elapid snakes, this underlines a drawback of current antivenom
 315 production based on immunized animal serum, since IgG has been shown to be the antibody
 316 isotype of therapeutic value (Fernandes et al., 2000). These findings therefore contribute to the
 317 understanding of snake toxin immunogenicity and indicate the difficulty in obtaining balanced
 318 immune responses in animals during the immunization process.

319

320 Acknowledgments

321 We thank Mikael Rørdam Andersen from the Technical University of Denmark for
322 fruitful scientific discussion. The following institutions and foundations are acknowledged for
323 supporting the research: Juno Therapeutics Inc., Instituto Clodomiro Picado, Universidad de
324 Costa Rica, and the Novo Nordisk Foundation (NNF13OC0005613 and NNF16OC0019248).

326 **References**

- 327 Alape-Girón A, Stiles B, Schmidt J, Girón-Cortés M, Thelestam M, Jörnvall H, Bergman T.
328 1996. Characterization of multiple nicotinic acetylcholine receptor-binding proteins and
329 phospholipases A₂ from the venom of the coral snake *Micrurus nigrocinctus nigrocinctus*.
330 *FEBS Letters* 380:29–32.
- 331 Antúnez J, Fernández J, Lomonte B, Angulo Y, Sanz L, Pérez A, Calvete JJ, Gutiérrez JM. 2010.
332 Antivenomics of *Atropoides mexicanus* and *Atropoides picadoi* snake venoms:
333 Relationship to the neutralization of toxic and enzymatic activities. *Journal of Venom*
334 *Research* 1:8–17.
- 335 Bolaños R, Cerdas L, Abalos JW. 1978. Venoms of coral snakes (*Micrurus* spp.): Report on a
336 multivalent antivenin for the Americas. *Bulletin of the Pan American Health Organization*
337 12:23–27.
- 338 Bucarety F, De Capitani EM, Vieira RJ, Rodrigues CK, Zannin M, Da Silva Jr. NJ, Casais-e-
339 Silva LL, Hyslop S. 2016. Coral snake bites (*Micrurus* spp.) in Brazil: A review of
340 literature reports. *Clinical Toxicology* 54:222–234.
- 341 Campbell JA, Lamar WW. 2004. *The Venomous Reptiles of the Western Hemisphere. Vol. II*.
342 Ithaca, New York: Comstock Publishing Associates, Cornell University Press.
- 343 Castro KL, Duarte CG, Ramos HR, de Avila RAM, Schneider FS, Oliveira D, Freitas CF,
344 Kalapothakis E, Ho PL, Chávez-Olortegui C. 2015. Identification and characterization of
345 B-cell epitopes of 3FTx and PLA₂ toxins from *Micrurus corallinus* snake venom. *Toxicon*
346 93:51–60.
- 347 Chotwiwatthanakun C, Ronachai P, Akesowan S, Sriprapat S, Ratanabanangkoon K. 2001.
348 Production of potent polyvalent antivenom against three elapid venoms using a low dose,

- 349 low volume, multi-site immunization protocol. *Toxicon* 39:1487–1494.
- 350 Cook DAN, Owen T, Wagstaff SC, Kinne J, Wernery U, Harrison RA. 2010. Analysis of
351 camelid IgG for antivenom development: serological responses of venom-immunised
352 camels to prepare either monospecific or polyspecific antivenoms for West Africa. *Toxicon*
353 56:363–372.
- 354 Corrêa-Netto C, Junqueira-de-Azevedo IL, Silva DA, Ho PL, Leitão-de-Araújo M, Alves ML,
355 Sanz L, Foguel D, Zingali RB, Calvete JJ. 2011. Snake venomomics and venom gland
356 transcriptomic analysis of Brazilian coral snakes, *Micrurus altirostris* and *M. corallinus*.
357 *Journal of Proteomics* 74:1795–1809.
- 358 Di Niro R, Lee SJ, Vander Heiden JA, Elsner RA, Trivedi N, Bannock JM, Gupta NT, Kleinstein
359 SH, Vigneault F, Gilbert TJ, Meffre E. 2015. *Salmonella* infection drives promiscuous B
360 cell activation followed by extrafollicular affinity maturation. *Immunity* 43:120–131.
- 361 Edgar RC. 2004. MUSCLE: multiple sequence alignment with high accuracy and high
362 throughput. *Nucleic Acids Research* 32:1792–1797.
- 363 Fernández J, Alape-Girón A, Angulo Y, Sanz L, Gutiérrez JM, Calvete JJ, Lomonte B. 2011.
364 Venomic and antivenomic analyses of the Central American coral snake, *Micrurus*
365 *nigrocinctus* (Elapidae). *Journal of Proteome Research* 10:1816–1827.
- 366 Fernandes I, Lima EX, Takehara HA, Moura-da-Silva AM, Tanjoni I, Gutiérrez JM. 2000. Horse
367 IgG isotypes and cross-neutralization of two snake antivenoms produced in Brazil and
368 Costa Rica. *Toxicon* 38:633–44.
- 369 Fernández J, Vargas N, Pla D, Sasa M, Rey-Suárez P, Sanz L, Gutiérrez JM, Calvete JJ,
370 Lomonte B. 2015. Snake venomomics of *Micrurus alleni* and *Micrurus mosquitensis* from the

- 371 Caribbean region of Costa Rica reveals two divergent compositional patterns in New
372 World elapids. *Toxicon* 107:217–233.
- 373 Guidolin RG, Marcelino RM, Gondo HH, Morais JF, Ferreira RA, Silva CL, Kipnis TL, Silva
374 JA, Fafetine J, da Silva WD. 2010. Polyvalent horse F(ab')₂ snake antivenom: development
375 of process to produce polyvalent horse F(ab')₂ antibodies anti-african snake venom. *African*
376 *Journal of Biotechnology* 9:2446–2455.
- 377 Gutiérrez JM, Lomonte B, Aird SD, da Silva Jr. NJ, 2016. Mecanismo de ação dos venenos de
378 cobras corais. In: *As Cobras Corais do Brasil: Biologia, Taxonomia, Venenos e*
379 *Envenenamientos* (da Silva Jr, N.J., Ed.), 415 pp. Editora PUC Goiás, GO, Brazil.
- 380 Gutiérrez JM, León G, Lomonte B, Angulo Y. 2011. Antivenoms for snakebite envenomings.
381 *Inflammation & Allergy Drug Targets* 10:369–380.
- 382 Gutiérrez JM, Sanz L, Flores-Díaz M, Figueroa L, Madrigal M, Herrera M, Villalta M, León G,
383 Estrada R, Borges A, Alape-Girón A, Calvete JJ. 2009. Impact of regional variation in
384 *Bothrops asper* venom on the design of antivenoms: Integrating antivenomics and
385 neutralization approaches. *Journal of Proteome Research* 9:564–577.
- 386 Judge RK, Henry PJ, Mirtschin P, Jelinek G, Wilce JA. 2006. Toxins not neutralized by brown
387 snake antivenom. *Toxicology and Applied Pharmacology* 213:117–125.
- 388 Lausten AH, Lomonte B, Lohse B, Fernández J, Gutiérrez JM. 2015. Unveiling the nature of
389 black mamba (*Dendroaspis polylepis*) venom through venomomics and antivenom
390 immunoprofiling: identification of key toxin targets for antivenom development. *Journal of*
391 *Proteomics* 119:126–142.

- 392 Laustsen AH, Engmark M, Milbo C, Johannesen J, Lomonte B, Gutiérrez JM, Lohse B. 2016.
393 From Fangs to Pharmacology: The Future of Snakebite Envenoming Therapy. *Current*
394 *Pharmaceutical Design* 22.
- 395 Laustsen AH, Solà M, Jappe EC, Oscoz S, Lauridsen LP, Engmark M. 2016. Biotechnological
396 trends in spider and scorpion antivenom development. *Toxins* 8:1–33.
- 397 Lomonte B, Sasa M, Rey-Suárez P, Bryan W, Gutiérrez JM. 2016a. Venom of the coral snake
398 *Micrurus clarki*: proteomic profile, toxicity, immunological cross-neutralization, and
399 characterization of a three-finger toxin. *Toxins* 8:138.
- 400 Lomonte B, Rey-Suárez P, Fernández J, Sasa M, Pla D, Vargas N, Bénard-Valle M, Sanz L,
401 Corrêa-Netto C, Núñez V, Alape-Girón A, Alagón A, Gutiérrez JM, Calvete JJ, 2016b.
402 Venoms of *Micrurus* coral snakes: evolutionary trends in compositional patterns emerging
403 from proteomic analyses. *Toxicon* (submitted).
- 404 Mardis ER. 2008. Next-generation DNA sequencing methods. *Annual Review of Genomics and*
405 *Human Genetics* 9:387–402.
- 406 Ownby C, Colberg T. 1990. Comparison of the immunogenicity and antigenic composition of
407 several venoms of snakes in the family Crotalidae. *Toxicon* 1990 28:189–199.
- 408 R Core Team (2014). R: A language and environment for statistical computing. R Foundation for
409 Statistical Computing, Vienna, Austria. URL <http://www.R-project.org/>.
- 410 Ramos HR, Junqueira-de-Azevedo ILM, Novo JB, Castro K, Duarte CG, Machado-de-Avila RA,
411 Chavez-Olortegui C, Ho PL. 2016. A heterologous multiepitope DNA prime/recombinant
412 protein boost immunisation strategy for the development of an antiserum against *Micrurus*
413 *corallinus* (coral snake) venom. *PLoS Neglected Tropical Diseases* 10:e0004484.

- 414 Rey-Suárez P, Núñez V, Gutiérrez JM, Lomonte B. 2011. Proteomic and biological
415 characterization of the venom of the redbellied coral snake, *Micrurus mipartitus* (Elapidae),
416 from Colombia and Costa Rica. *Journal of Proteomics* 75:655–667.
- 417 Rey-Suárez P, Stuani-Floriano R, Rostelato-Ferreira S, Saldarriaga M, Núñez V, Rodrigues-
418 Simioni L, Lomonte B. 2012. Mipartoxin-I, a novel three-finger toxin, is the major
419 neurotoxic component in the venom of the redbellied coral snake *Micrurus mipartitus*
420 (Elapidae). *Toxicon* 60:851–863.
- 421 Rey-Suárez P, Núñez V, Fernández J, Lomonte B. 2016. Integrative characterization of the
422 venom of the coral snake *Micrurus dumerilii* (Elapidae) from Colombia: proteome,
423 toxicity, and cross-neutralization by antivenom. *Journal of Proteomics* 136:262–273.
- 424 Rosso JP, Vargas-Rosso O, Gutiérrez JM, Rochat H, Bougis PE. 1996. Characterization of α -
425 neurotoxin and phospholipase A₂ activities from *Micrurus* venoms. *European Journal of*
426 *Biochemistry* 238:231–239.
- 427 Sanz L, Pla D, Pérez A, Rodríguez Y, Zavaleta-Martínez A, Salas M, Lomonte B, Calvete JJ.
428 2016. Venomic analysis of the poorly studied desert coral snake, *Micrurus tschudii*
429 *tschudii*, supports the 3FTx/PLA₂ dichotomy across *Micrurus* venoms. *Toxins* 8:178.
- 430 Schottler WH. 1951. Antigen-antibody relations in the present antivenin production of Brazil.
431 *American Journal of Tropical Medicine and Hygiene* 31:500–509.
- 432 Stern JN, Yaari G, Vander Heiden JA, Church G, Donahue WF, Hintzen RQ, Huttner AJ, Laman
433 JD, Nagra RM, Nylander A, Pitt D. 2014. B cells populating the multiple sclerosis brain
434 mature in the draining cervical lymph nodes. *Science Translational Medicine* 6:248ra107.

- 435 Tanaka G, Furtado MFD, Portaro FCV, Sant'Anna OA, Tambourgi DV. 2010. Diversity of
436 *Micrurus* snake species related to their venom toxic effects and the prospective of
437 antivenom neutralization. *PLoS Neglected Tropical Diseases* 4:622.
- 438 Tanaka GD, Sant'Anna OA, Marcelino JR, da Luz ACL, da Rocha MMT, Tambourgi DV. 2016.
439 *Micrurus* snake species: venom immunogenicity, antiserum cross-reactivity and
440 neutralization potential. *Toxicon* 117:59–68.
- 441 Tsioris K, Gupta NT, Ogunniyi AO, Zimnisky RM, Qian F, Yao Y, Wang X, Stern JN, Chari R,
442 Briggs AW, Clouser CR. 2015. Neutralizing antibodies against West Nile virus identified
443 directly from human B cells by single-cell analysis and next generation sequencing.
444 *Integrative Biology* 7:1587–1597.
- 445 Vander Heiden JA, Yaari G, Uduman M, Stern JN, O'Connor KC, Hafler DA, Vigneault F,
446 Kleinstein SH. 2014. pRESTO: a toolkit for processing high-throughput sequencing raw
447 reads of lymphocyte receptor repertoires. *Bioinformatics* 30:1930–1932
- 448 Vergara I, Pedraza-Escalona M, Paniagua D, Restano-Cassulini R, Zamudio F, Batista CV,
449 Possani L., Alagón A. 2014. Eastern coral snake *Micrurus fulvius* venom toxicity in mice is
450 mainly determined by neurotoxic phospholipases A₂. *Journal of Proteomics* 105:295–306.
- 451 Walsh G. 2014. Biopharmaceutical benchmarks 2014. *Nature biotechnology* 32:992–1000.
- 452 Warrell DA. 2010. Snake bite. *Lancet* 375:77–88.
- 453 Warrell DA. 2004. Snakebites in Central and South America: Epidemiology, clinical features
454 and clinical management. In: Campbell JA, Lamar WW, Eds. *The Venomous Reptiles of the*
455 *Western Hemisphere. Vol. II.* Ithaca, New York: Comstock Publishing Associates, Cornell
456 University Press, 709–761.

457 Williams DJ, Gutiérrez JM, Calvete JJ, Wüster W, Ratanabanangkoon K, Paiva O, Brown NI,
458 Casewell NR, Harrison RA, Rowley PD, O'Shea M. 2011. Ending the drought: new
459 strategies for improving the flow of affordable, effective antivenoms in Asia and Africa.
460 *Journal of Proteomics* 74:1735–1767.

461 Ye J, Ma N, Madden TL, Ostell JM. 2013. IgBLAST: an immunoglobulin variable domain
462 sequence analysis tool. *Nucleic Acids Research* 41:W34-W40.

463